Molybdate Inhibits Hsp90, Induces Structural Changes in Its C-Terminal Domain, and Alters Its Interactions with Substrates†

Steven D. Hartson,*,‡ Vanitha Thulasiraman,‡,§ Wenjun Huang,‡ Luke Whitesell,|| and Robert L. Matts‡

Department of Biochemistry and Molecular Biology, Oklahoma State University, Stillwater, Oklahoma 74078-3035, and Steele Memorial Children's Research Center, University of Arizona, Tucson, Arizona 85724

Received December 23, 1998

ABSTRACT: To examine the biochemical mechanism by which hsp90 exerts its essential positive function on certain signal transduction proteins, we characterized the effects of molybdate and geldanamycin on hsp90 function and structure. Molybdate inhibited hsp90-mediated p56^{lck} biogenesis and luciferase renaturation while enforcing salt-stable interactions with these substrates. Molybdate also reduced the amount of free hsp90 present in cell lysates, inhibited hsp90's ability to bind geldanamycin, and induced resistance to proteolysis at a specific region within the C-terminal domain of hsp90. In contrast, the hsp90 inhibitor geldanamycin prevented hsp90 from assuming natural or molybdate-induced conformations that allow salt-stable interactions with substrates. When these compounds were applied sequentially, the order of addition determined the effects observed, indicating that these agents had opposing effects on hsp90. We conclude that a specific region within the C-terminal domain of hsp90 (near residue 600) determines the mode by which hsp90 interacts with substrates and that the ability of hsp90 to cycle between alternative modes of interaction is obligatory for hsp90 function.

Nucleotide-modulated conformational changes allow molecular chaperones of the DnaK and GroEL families to facilitate a variety of important and essential folding events that occur during the life cycle of a protein (for reviews, see refs *1*−*6*). For the DnaK/hsp70[1] chaperones, occupancy of their nucleotide-binding pocket by ADP is accompanied by a "closed" or "slow-on, slow-off" chaperone conformation. In this conformation, the chaperone binds tightly to hydrophobic polypeptide motifs exposed on the surfaces of protein folding intermediates. Conversely, when ATP occupies the nucleotide-binding pocket, the chaperone exhibits an "open" or "fast-off, fast-on" conformation. In this alternative conformation, the chaperone does not bind tightly to the protein folding intermediate, and the folding intermediate is free to attempt to fold in an aqueous environment. Switching between these contrasting conformations is mediated by nucleotide hydrolysis or exchange, and these processes are in turn regulated by allosteric contributions from accessory proteins which may themselves provide chaperone activity (e.g., DnaJ). Like that by the DnaK/hsp70 family of chaperones, binding and release of substrates by GroEL/GroES are mediated by regulated nucleotide binding, hydrolysis, and exchange. Thus, for both families of chaperones, reversible interactions between chaperones and their substrates allow protein folding intermediates to search complicated free energy topologies while minimizing nonproductive protein folding pathways.

Evidence suggests that the 90 kDa chaperones (hsp90) also require ATP to facilitate the in vivo folding of certain proteins, especially those mediating cellular signal transduction events. In rabbit reticulocyte lysates (RRL), ATP is required for the efficient assembly of heterocomplexes between hsp90 and salt-stripped steroid hormone receptors or protein kinases (*7*). Similarly, ATP is required in RRL for hsp90-mediated renaturation of heat-denatured firefly luciferase (*8*−*10*). Additionally, ATP is required for the association of hsp90 with its p23 ancillary protein (or "cohort") both in unfractionated rabbit reticulocyte lysates (*11*−*14*) and in assays in which purified components are being used (*15*). In addition to requiring ATP, the association of hsp90 with p23 is stabilized by molybdate (*16*), a metal ion that also stabilizes hsp90's interactions with steroid hormone receptors and with certain kinases (for review, see ref *17*). The belief that ATP mediates hsp90 function is further supported by cocrystallization and structural characterization of a complex formed between the N-terminal domain of hsp90 and adenine nucleotides; this structure reveals a distinct nucleotide-binding pocket within this domain of hsp90 (*18*). Consistent with this structure, the N-terminal domain of hsp90 directly binds to γ-linked ATP−

† This work was supported by grants from the Oklahoma Center for Advancement of Science and Technology (HN6-018 to S.D.H.), the National Institute of General Medicine, NIH (GM51608 to R.L.M.), the National Institute of Environmental Health Sciences, NIH (ES04299 to R.L.M.), and the National Cancer Institute, NIH (CA59537-03 to L.W.) and by the Oklahoma Agricultural Experiment Station (Project 1975).

* Corresponding author: 246 NRC, Department of Biochemistry and Molecular Biology, Oklahoma State University, Stillwater, OK 74078-3035. Telephone: (405) 744-9330. Fax: (405) 744-7799. E-mail: shartson@bmb-fs1.biochem.okstate.edu.

‡ Oklahoma State University.

§ Present address: Department of Biological Sciences, Stanford University, Stanford, CA 94305.

|| University of Arizona.

[1] Abbreviations: hsp, heat shock protein; RRL, rabbit reticulocyte lysate, typically supplemented with the salts and an ATP-regenerating system necessary to support in vitro protein synthesis; p56^{lck}F505, mutant form (Y505 → F) of the 56 kDa lymphoid cell kinase.

10.1021/bi983027s CCC: $18.00
Published on Web 03/05/1999

Sepharose, and mutation of glycine residues of an ATP-binding motif within this domain reduces the extent of hsp90's ATP-dependent interaction with p23 (*19*). Additionally, electron spin resonance spectroscopy can detect weak interactions between full-length hsp90 and spin-labeled ATP analogues (*20*). However, although these observations document a role for ATP in hsp90 function, the roles played by adenosine nucleotides during hsp90-mediated processes are poorly understood.

In addition to binding adenosine nucleotide, the N-terminal nucleotide-binding pocket of hsp90 is also the site to which the benzoquinonoid ansamycin geldanamycin binds (*21*). This binding disrupts the physical interaction of hsp90 with viral $p60^{src}$ and indirectly compromises the function of this kinase (*22*). Subsequently, geldanamycin has been found to disrupt the function of numerous other hsp90-dependent proteins by altering their normal interactions with hsp90 machinery. Specifically, geldanamycin prevents the recovery of p23 in hsp90·substrate complexes (*16*, *23*), and it has been suggested that the absence of the p23 cohort from geldanamycin-treated hsp90 heterocomplexes reflects a role for p23 in stabilizing interactions between hsp90 and its substrates (*14*). The absence of p23 from geldanamycin-treated hsp90 heterocomplexes appears to be a direct consequence of geldanamycin treatment, as geldanamycin inhibits the association of hsp90 with its p23 cohort in unfractionated cell lysates (*11*) and in assays in which purified components are being used (*15*). While it is well understood that the binding of geldanamycin within the nucleotide-binding pocket of hsp90 affects the function and stability of hsp90 substrates and alters the composition of hsp90 heterocomplexes, the biochemical mechanism by which this novel anticancer agent inhibits hsp90 function is poorly understood.

Relevant to questions regarding the role of ATP in hsp90-mediated protein folding and the mechanism of geldanamycin action, Toft and co-workers have presented evidence that nucleotide binding at the N-terminal domain of hsp90 mediates switching of hsp90 between two conformations (*15*, *19*). This model is based on a set of three complementary observations. (i) ATP and geldanamycin bind to the N-terminal domain of hsp90 (*18*, *19*, *21*). (ii) These compounds modulate the interaction of hsp90 with p23 and with hydrophobic chromatography resins (*15*, *24*). (iii) Hsp90 appears to interact with p23 and with hydrophobic resins at sites distal to the N-terminal domain of hsp90 (unpublished observations of D. O. Toft et al., cited in ref *19*). Thus, nucleotides and geldanamycin bind to the N-terminus of hsp90 and alter protein−protein interactions which occur at sites distal to the N-terminus, suggesting that such binding mediates global changes in hsp90's conformation. According to the model proposed by Toft and co-workers, hsp90 has a conformation that simultaneously binds p23 and ATP (or p23 and an ADP−molybdate complex). The model also proposes a second conformation for hsp90 capable of simultaneously binding phenyl-Sepharose and ADP (or phenyl-Sepharose and geldanamycin). Consistent with this model, binding of geldanamycin to hsp90 alters the conformation of hsp90 within the immediate vicinity of the geldanamycin-binding pocket (*21*). However, the specific global conformational changes that hsp90 might undergo and the effects of these conformations on the interaction of hsp90 with its substrates are unknown. Our current understanding of these aspects of hsp90 function is the subject of a recent review (*25*).

To examine the biochemical mechanism by which hsp90 exerts its essential positive function on certain signal transduction proteins, we characterized the effects of geldanamycin and molybdate on hsp90's physical and functional interactions with two of its previously characterized substrates, heat-denatured luciferase (*8*−*10*) and the tyrosine kinase $p56^{lck}$ (*26*−*28*). We also examined the effects of these agents on hsp90's structure. Results demonstrate that molybdate and geldanamycin both inhibited hsp90 function. Order-of-addition experiments indicated that molybdate and geldanamycin had opposing effects on hsp90, enforcing hsp90 structures with high and low affinities for substrates, respectively. Additionally, molybdate conveyed protease resistance to a specific region within the C-terminal domain of hsp90 that was normally highly susceptible to proteolysis. These results indicate that structural changes at a specific C-terminal region of hsp90 determine two modes by which hsp90 interacts with substrates, and that both modes are essential for hsp90 function.

EXPERIMENTAL PROCEDURES

Reagents. Three anti-hsp90 antibodies were used to detect full-length hsp90 and proteolytic fragments of hsp90. (i) The AC88 monoclonal antibody recognizes the C-terminus of hsp90 (*29*−*31*) and was obtained from Stressgen. (ii) Affinity-purified polyclonal rabbit antibodies raised against a peptide representing the N-terminus of mouse hsp86 were obtained from Affinity BioReagents, Inc. (iii) Polyclonal "8486" antiserum isolated from rabbits immunized with full-length purified hsp90 (*32*) was obtained from S. J. Ullrich (National Cancer Institute, Bethesda, MD). For immunoadsorption of firefly luciferase, affinity-purified polyclonal rabbit antibodies recognizing full-length firefly luciferase were obtained from Promega Corp. Polyclonal mouse antibodies against $p56^{lck}$ were prepared as described elsewhere.[2] Geldanamycin was obtained from the Drug Synthesis and Chemistry Branch, Developmental Therapeutics Program, Division of Cancer Treatment, National Cancer Institute. Molybdate was prepared as a 0.2 or 0.4 M stock immediately before use; alternatively, molybdate stocks were stored as single-use aliquots at −20 °C. Buffers used to wash immunoadsorptions included 10 mM Tris·HCl at pH 7.4 (TB); 10 mM Tris·HCl and 50 mM NaCl at pH 7.4 (TB50); 10 mM Tris·HCl and 150 mM NaCl at pH 7.4 (TB150); 10 mM Tris·HCl and 500 mM NaCl at pH 7.4 (TB500); 10 mM PIPES·NaOH, 150 mM NaCl, and 0.05% Tween 20 at pH 7.0 (P150T); and 10 mM PIPES·NaOH and 500 mM NaCl at pH 7.0 (P500). These buffers contained or lacked 10 mM sodium molybdate, as indicated.

Inhibition of Hsp90 Function by Molybdate. $p56^{lck}$ was synthesized and radiolabeled with [^{35}S]Met by coupled transcription and translation in nuclease-treated rabbit reticulocyte lysate as previously described (*26*, *27*). Protein synthesis was assessed by determination of the extent of [^{35}S]-Met incorporation into TCA-insoluble protein; such an assessment indicated that molybdate inhibited polypeptide elongation when added to protein synthesis mixes. Thus, to

[2] P. Yorgin et al., submitted for publication.

determine the effects of molybdate on hsp90-mediated biogenesis, $p56^{lck}$ was synthesized for 17 min in the absence of molybdate, after which aurin tricarboxylic acid (ATA) was added to inhibit the reinitiation of protein synthesis (75 μM final concentration). Polyribosomes were allowed to run off for an additional 7 min, after which molybdate was added to a 20 mM final concentration. Reaction mixtures were then either flash-frozen in liquid nitrogen or subjected to maturational incubations for 1−2 h further before flash-freezing. Immunoadsorption mixtures were washed four times with P150T and once with P500. $p56^{lck}$ kinase activity was assessed as described previously (*33*). To determine the effects of molybdate on the hsp90-mediated renaturation of luciferase, kinetic analyses of luciferase renaturation in drug-treated RRL were performed as previously described (*10*); each kinetic analysis was repeated a minimum of three times.

To determine the effects of geldanamycin and/or molybdate on the luciferase·hsp90 complex, luciferase (40 μg) was denatured at 41 °C for 10 min and adsorbed for 2 h at 4 °C to affinity-purified anti-luciferase antibody (4 μL) bound to goat anti-rabbit immunoresins prepared as described previously (*34*). Control reaction mixtures received no luciferase. After binding, the luciferase immunocomplex was washed with TB150, TB500, TB150, and TB50. The luciferase immunocomplex was subsequently mixed for 20 min at 30 °C in protein folding reaction mixtures containing 50% (v/v) rabbit reticulocyte lysate, an ATP-regenerating system (10 mM creatine phosphate and 20 units/mL creatine phosphokinase), and 75 mM KCl. These reaction mixtures also contained geldanamycin (1 μg/mL), Me_2SO_4 (geldanamycin vehicle control), and/or sodium molybdate (20 mM) as indicated. After incubation, the immunocomplex and adsorbed proteins were separated from unadsorbed proteins by centrifugation. Pellets were washed four times with TB50 (low-salt wash), or alternatively, immunocomplexes were washed once with TB50, three times with TB500, and once with TB50 (high-salt wash). For washing of immunocomplexes formed in the presence of molybdate, 10 mM molybdate was included in all wash buffers. Immunoadsorbed proteins were eluted by boiling in SDS−PAGE sample buffer and analyzed by SDS−PAGE and Western blotting with "8486" rabbit antiserum (see Reagents).

Effects of Geldanamycin on Hsp90−Substrate Interactions. To assess the effects of geldanamycin on interactions between hsp90 and $p56^{lck}$, $p56^{lck}$ was synthesized for 30 min in RRL containing geldanamycin and/or Me_2SO_4 vehicle (5 μg/mL and 0.5% final concentrations, respectively). Complexes between $p56^{lck}$ and hsp90 were co-immunoadsorbed with 5 μL of polyclonal mouse anti-$p56^{lck}$ ascites fluid bound to a 15 μL bed volume of goat anti-(mouse IgG) immunoresin (*34*). Immunoadsorption mixtures from 70 μL of protein synthesis reaction mixtures were washed three times with TB, once with either TB (low-salt wash) or with TB500 (high-salt wash), and twice again with TB. Immunoadsorbed proteins were eluted by boiling in SDS−PAGE sample buffer and analyzed by SDS−PAGE and Western blotting with rabbit antibodies directed against the N-terminus of mouse hsp86.

Effects of Molybdate and Geldanamycin on Hsp90 Structure. Rabbit reticulocyte lysate reaction mixtures contained 50% (v/v) rabbit reticulocyte lysate, an ATP-regenerating system (10 mM creatine phosphate and 20 units/mL creatine phosphokinase), and 75 mM KCl and were incubated for 5 min at 37 °C in the presence of either 20 mM sodium molybdate, 5 μg/mL geldanamycin, or drug vehicle (water or 0.5% Me_2SO_4). For sequential drug applications, the second drug was applied after preincubation with the first drug and reaction mixtures were incubated for a further 5 min.

After drug treatments, the reaction mixtures were chilled on ice and used in geldanamycin binding assays as previously described (*22*). Alternatively, AC88 anti-hsp90 monoclonal mouse IgG (2.0 μg) was immobilized on goat anti-mouse immunoresins (*34*), and immunoresins were washed twice in TB150. These immunoresins (15 μL packed volume) were incubated with 2.0 μL aliquots of drug-treated RRL reaction mixtures for 2.5 h. After binding, immunoresins were suspended in 100 μL of TB150 and pelleted by centrifugation, and the supernatant containing unbound proteins was analyzed by SDS−PAGE and Western blotting with rabbit antibodies directed against the N-terminus of hsp90. Additionally, immunoadsorbed pellets were assessed similarly by Western blotting after the washing of immunoresins.

To directly detect altered hsp90 structure resulting from treatment with molybdate and/or geldanamycin, reaction mixtures were assembled and treated as described above. After drug treatment, reaction mixtures were chilled on ice and the desired concentrations of TPCK-treated trypsin (Worthington) were applied as 2× stocks in TB150 containing 4 mM $CaCl_2$ and 0.1 mM EDTA. After digestion on ice for 6 min, reactions were stopped by immediate boiling in SDS−PAGE sample buffer, and digestion products were analyzed by SDS−PAGE and Western blotting with either rabbit antibodies directed against the N-terminus of mouse hsp86 or with AC88 anti-hsp90 monoclonal antibody.

RESULTS

Effects of Molybdate on Hsp90-Mediated Folding Processes. Some models for hsp90 function suggest that physical association with hsp90 specifies competent or active protein conformations (*35*). These models are based primarily on observations regarding the heterocomplex formed between hsp90 and hsp90-dependent steroid hormone receptors (for review, see ref *17*). At physiological temperatures, these receptors require hsp90 function to assume conformations competent to bind hormone, and this competence is maintained in receptor·hsp90 heterocomplexes stabilized by molybdate. In addition to steroid receptors, hsp90 plays an essential positive role for several hsp90-associated kinases, including $p56^{lck}$ (*26*−*28*), viral $p60^{src}$ (*22*, *36*), raf (*37*−*40*), and the heme-regulated eIF-2α kinase (*34*, *41*, *42*). These kinases exhibit moderate kinase activity when isolated as complexes with hsp90; however, these activities are typically smaller than those observed for the free kinases. Inhibition of hsp90 function by geldanamycin has been found to result in production of atypical or undetectable kinase·hsp90 heterocomplexes and to produce kinase molecules whose phosphotransferase activity and resistance to mild proteolysis are compromised. Thus, findings to date support models of hsp90 function in which hsp90 acts in a fashion analogous to that of a regulatory subunit to stabilize intermediate active conformations of certain signal transduction molecules.

To test this model, the effects of molybdate on the association of hsp90 with $p56^{lck}$ were assessed following

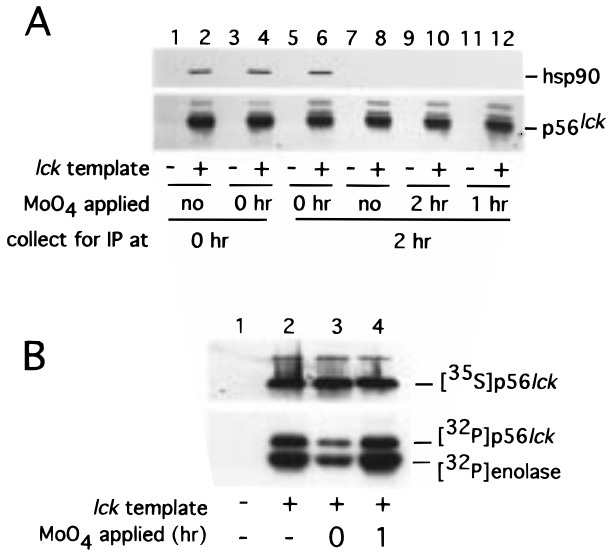

FIGURE 1: Effect of molybdate on p56^{lck} maturation. (A) In vitro translation reactions were (even-numbered lanes), or were not (odd-numbered lanes), programmed for a brief synthesis of p56^{lck}. After arrest of protein synthesis and a 7 min runoff of polyribosomes, protein synthesis reaction mixtures either were immunoadsorbed immediately and (lanes 1−4) or were immunoadsorbed after a 2 h maturation at 37 °C (lanes 5−12). Immunoadsorbed materials were analyzed by Western blotting with anti-p56^{lck} and anti-hsp90 antibodies: lanes 1, 2, 7, and 8, analysis of p56^{lck} maturation in the absence of molybdate; lanes 3, 4, 9, and 10, molybdate added to chilled protein synthesis reaction mixtures immediately before immunoadsorption; lanes 5 and 6, molybdate added immediately after polyribosome runoff, after which reactions were allowed to mature for a further 2 h at 37 °C; and lanes 11 and 12, kinase molecules allowed to mature at 37 °C for 1 h in the absence of molybdate, after which molybdate was added and reaction mixtures were further incubated for an additional 1 h at 37 °C. (B) In vitro kinase assays were used to assess kinase activity produced in p56^{lck}-F505 maturation reaction mixtures to which molybdate was added prior to (lane 3) or after (lane 4) the 1 h posttranslational maturation at 30 °C. A control reaction mixture lacking *lck* template was also analyzed (lane 1). Reaction mixtures were immunoadsorbed with anti-p56^{lck} antibodies, and immunoresins were assayed in the presence of acid-denatured enolase and [γ-^{32}P]ATP. In the upper panel, aliquots of the immunoadsorption mixtures were analyzed by SDS−PAGE and autoradiography to assess immunoadsorption efficiency. In the lower panel, products of the kinase reaction were assessed by SDS−PAGE and autoradiography.

synthesis of p56^{lck} in RRL and coadsorption of the hsp90·p56^{lck} heterocomplex with anti-p56^{lck} antibodies. Immediately after p56^{lck} synthesis, anti-p56^{lck} antibodies specifically co-immunoadsorbed an hsp90·p56^{lck} heterocomplex (Figure 1A, lane 2). When protein synthesis was arrested and the translation and/or folding reaction carried out further at 37 °C for 2 h, the amount of hsp90 detected in association with p56^{lck} declined to undetectable levels (Figure 1A, lane 8); this result was consistent with previous demonstrations of transient interactions between hsp90 and wild-type p56^{lck} (*27*, *28*) or between hsp90 and viral p60^{src} (*43*, *44*). The transient nature of this interaction was not affected by the addition of molybdate to mature p56^{lck} reactions immediately prior to the immunoadsorption procedure (Figure 1A, lane 10). Nor did prolonged incubation in the presence of molybdate induce the association of hsp90 with p56^{lck} molecules if kinase molecules first matured in the absence of molybdate (Figure 1A, lane 12). In contrast, addition of molybdate to RRL folding reaction mixtures immediately after p56^{lck} synthesis, but prior to completion of de novo folding, slightly increased the amount of hsp90 coadsorbed with immature p56^{lck} (Figure 1A, lane 4) and prevented the decline in the number of hsp90·p56^{lck} associations that normally accompanied maturation of wild-type kinase molecules at 37 °C (Figure 1A, lane 6). Equivalent results were observed when the maturation of the F505 regulatory mutant of p56^{lck} (*28*) was examined in molybdate-treated reaction mixtures incubated at 30 °C (not shown). These results were consistent with previous demonstrations that molybdate stabilized the physical association of hsp90 with a variety of hsp90-dependent kinases (*45*). Furthermore, these results indicated that the effect of molybdate was not a simple stabilization of an isolated kinase·hsp90 heterocomplex, but rather suggested that in ATP-replete RRL, molybdate inhibited the normal flow of p56^{lck} molecules from an hsp90-bound state to hsp90-free forms.

To test the hypothesis that physical association with hsp90 was adequate to generate and stabilize p56^{lck} in an active conformation, we assessed the phosphotransferase activity of p56^{lck} molecules that matured in the presence or absence of molybdate. A mutant form of p56^{lck} (p56^{lck}F505) encoding phenylalanine at position 505 (*46*) was used in these studies to eliminate ambiguities regarding the effects of molybdate on the dephosphorylation of the negative regulatory tyrosine normally found in this position. Addition of molybdate to chilled p56^{lck}F505 RRL mixtures whose reactions were mature just prior to immunoadsorption did not inhibit p56^{lck}-F505 activity detected in subsequent kinase assays (Figure 1B, lane 2 vs 4). Nor did incubation of p56^{lck}F505 in molybdate-treated RRL result in loss of p56^{lck}F505 activity when this kinase first matured in untreated RRL (not shown). In contrast, maturation of newly synthesized p56^{lck}F505 molecules in molybdate-treated RRL significantly compromised the net kinase activity of the population of p56^{lck}F505 molecules thus produced (Figure 1B, lane 3 vs 2). The magnitude of this decrease (70% decrease in kinase specific activity) was comparable to that produced during equivalent maturation of p56^{lck} in the presence of geldanamycin (*27*). These results demonstrated that the thesis hypothesis was incorrect; the simple association of p56^{lck}F505 with hsp90 was inadequate to generate fully active kinase molecules. These results further suggested that molybdate's inhibition of the normal flow of p56^{lck} molecules from an hsp90-bound state to an hsp90-free state (Figure 1A) was accompanied by an inhibition of the essential positive function that hsp90 normally supplied during kinase biogenesis.

To determine if molybdate inhibited other hsp90-dependent folding processes, we investigated the effect of molybdate on the renaturation of thermally denatured firefly luciferase, a process which is normally facilitated by hsp90 chaperone machinery in RRL (*10*). The effects of increasing concentrations of molybdate on luciferase renaturation were assessed in RRL reaction mixtures containing constant saturating concentrations of ATP and a limiting concentration of denatured luciferase of 8 nM (Figure 2A). Molybdate inhibited the renaturation of luciferase in a concentration-dependent manner with an IC_{50} of ~5 mM. Nearly complete inhibition of the renaturation of 8 nM luciferase was observed in the presence of 100 mM molybdate. These findings supported results obtained regarding the effects of molybdate on kinase biogenesis, namely, that molybdate was an inhibitor of hsp90-dependent protein folding processes.

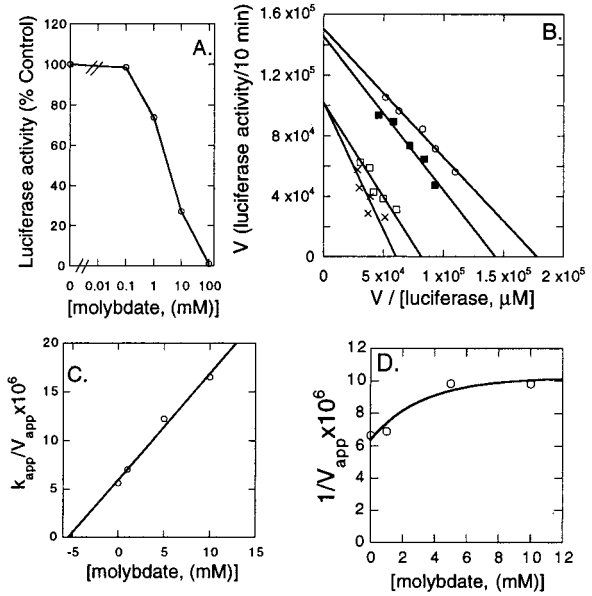

FIGURE 2: Effect of molybdate on luciferase renaturation in undialyzed RRL. (A) Concentration dependence for molybdate-induced inhibition of luciferase renaturation in RRL. Heme-deficient protein synthesis mixes (100 μL) containing 10 μM edeine were preincubated for 20 min at 30 °C in the presence of 0, 0.1, 1.0, 10, or 100 mM molybdate. Five microliters of denatured luciferase (10 μg/mL) was then diluted into 100 μL of lysate. After 10 min, the amount of luciferase activity present in a 20 μL aliquot of each reaction mixture was measured. Luciferase activity is reported as a percentage of the activity present in the control containing no molybdate. (B) Kinetic analysis of the effect of molybdate on chaperone-mediated luciferase renaturation in RRL. The rate of luciferase renaturation (V in light-forming units renatured in 10 min) was measured at saturating (1.7 mM endogenous) ATP and varying luciferase concentrations (2.0, 1.5, 1.0, 0.77, and 0.51 μM) in heme-deficient protein synthesis mixes containing no molybdate (○), 1 mM molybdate (■), 5 mM molybdate (□), or 10 mM molybdate (×) as described in Experimental Procedures. Shown is a Eadie−Hofstee plot of the data. The experiment was repeated three times with similar results. (C) Replot of k_{app}/V_{app} vs molybdate concentration. (D) Replot of $1/V_{app}$ vs molybdate concentration.

To further investigate the mechanism by which molybdate inhibited luciferase renaturation, the effects of molybdate on the kinetics of luciferase renaturation in RRL were determined under conditions which we have previously used to characterize the mechanism of action of the hsp90-specific inhibtor geldanamycin (*10*). The initial rates of luciferase renaturation were assessed in RRL reaction mixtures containing constant saturating concentrations of ATP and various concentrations of hsp90 substrate (0.5−2.0 μM denatured luciferase) and molybdate (0−10 mM molybdate) (Figure 2B). Eadie−Hofstee plots of the data indicated that molybdate was a noncompetitive inhibitor of luciferase renaturation with respect to the substrate heat-denatured luciferase, affecting both the V_{app} and V_{app}/k_{app} of the reaction. Replots of molybdate concentration versus k_{app}/V_{app} appeared to be linear over the range of molybdate concentrations examined and yielded an estimated K_i value of ~5 mM molybdate (Figure 2C). However, the best fits for replots of molybdate concentration versus $1/V_{app}$ were hyperbolic (Figure 2D), indicating that at saturating luciferase concentrations, luciferase renaturation could not be completely inhibited even at "infinite" molybdate concentrations. This latter result indicated that an alternative molybdate-resistant pathway for luciferase renaturation existed in RRL; this result was

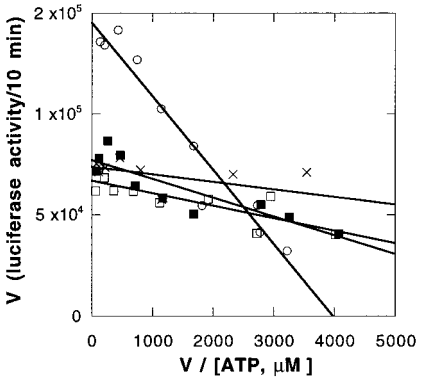

FIGURE 3: Eadie−Hofstee plot of the effects of molybdate on the kinetics of luciferase renaturation in the presence of varying ATP concentrations. The kinetics of luciferase renaturation were measured at near-saturating luciferase and varying ATP and molybdate concentrations. The rate of luciferase renaturation was measured in 100 μL of dialyzed lysate containing 2.1 μM luciferase and varying (10 μM to 1.0 mM) ATP concentrations in the presence of no molybdate (○), 5 mM molybdate (■), 10 mM molybdate (□), or 20 mM molybdate (×).

consistent with our previous presentation of evidence for an alternative, kinetically slower pathway for luciferase renaturation in RRL that could not be inhibited by the hsp90-binding drug geldanamycin (*10*).

Kinetic characterizations of luciferase renaturation were also performed in dialyzed RRL in which the concentration of ATP was varied by buffering with a creatine kinase/creatine phosphate ATP-regenerating system (Figure 3). In the presence of near-saturating concentrations of denatured luciferase, molybdate was found to be a noncompetitive inhibitor of luciferase renaturation with regard to ATP. Replots of molybdate concentration versus k_{app}/V_{app} or $1/V_{app}$ appeared to be nonlinear (not shown). For three independent data sets examined, the best fits for replots of molybdate concentration versus k_{app}/V_{app} or $1/V_{app}$ were parabolic, but the difficulties inherent to simultaneous multicondition kinetic analyses of sets of ATP-buffered RRL did not permit the collection of data that would have provided a rigorous exclusion of a linear fit. A parabolic fit of the replots would have been expected if two molecules of molybdate were binding to each hsp90 chaperone machine (an interpretation consistent with the widely held belief that hsp90 functions a dimer).

Molybdate caused a significant reduction in the estimated k_{app} for ATP for the renaturation of luciferase. In four independent experiments in which the effects of varying concentrations of ATP in the presence of near-saturating concentrations of luciferase were examined, 10 mM molybdate decreased the k_{app} for ATP by 74 ± 4% (from 46 ± 12 μM in uninhibited RRL to 12 ± 5 μM in molybdate-treated RRL). This molybdate-induced reduction in the k_{app} for ATP resulted in a stimulation of the rate of luciferase renaturation at low concentrations of ATP above that observed in the absence of molybdate. Since the lowest concentration of ATP we were able to obtain upon dialysis of RRL was 10−15 μM, the initial velocity of luciferase renaturation rapidly approached the V_{app} for the reaction as ATP concentrations were increased in the presence of molybdate. This effect of molybdate resulted in the generation of nearly horizontal lines for the Eadie−Hofstee plots, making an accurate estimation of the k_{app} for ATP for the reaction difficult. Nonetheless,

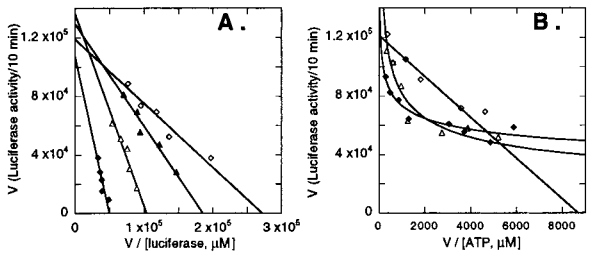

FIGURE 4: Effect of phosphate on the rate of luciferase renaturation. (A) The rate of luciferase renaturation was measured in 100 μL of dialyzed lysate containing 1.0 mM ATP, a creatine kinase/creatine phosphate ATP-regenerating system, and varying luciferase concentrations (1.5, 1.0, 0.75, 0.51, and 0.25 μM). Reaction mixtures contained no phosphate (◇), 40 mM phosphate (▲), 60 mM phosphate (△), or 80 mM phosphate (◆). (B) The kinetics of luciferase renaturation were measured at near-saturating luciferase and varying ATP and molybdate concentrations. The rate of luciferase renaturation was measured in 100 μL of dialyzed lysate containing 2.1 μM luciferase and varying (10−330 μM) ATP concentrations in the presence of no phosphate (◇), 60 mM phosphate (△), or 80 mM phosphate (◆).

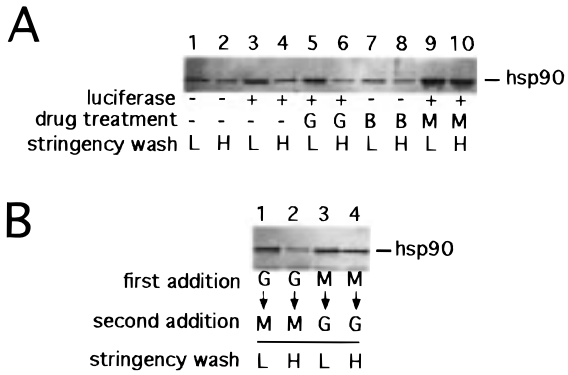

FIGURE 5: Effect of molybdate on the salt stability of the heterocomplex formed between hsp90 and heat-denatured luciferase. (A) Anti-luciferase immunoresins were (lanes 3−6, 9, and 10), or were not (lanes 1, 2, 7, and 8), incubated with heat-denatured firefly luciferase and subsequently incubated in RRL folding reaction mixtures containing either the drug vehicle Me_2SO_4 (lanes 1−4, 9, and 10), geldanamycin (G; lanes 5 and 6), molybdate (M; lanes 9 and 10), or both drugs applied simultaneously (B; lanes 7 and 8). After incubation for 20 min at 30 °C, immunopellets were washed with either low-salt buffer (L; odd-numbered lanes) or high-salt buffer (H; even-numbered lanes). Washed immunopellets were eluted in SDS−PAGE sample buffer and analyzed by Western blotting with anti-hsp90. (B) The effects of sequential applications of geldanamycin and molybdate on the subsequent salt resistance of the luciferase•hsp90 heterocomplex were analyzed as described for panel A. For sequential additions, lysates were preincubated for 10 min at 30 °C with either geldanamycin (lanes 1 and 2) or molybdate (lanes 3 and 4), after which a second drug treatment with either molybdate (lanes 1 and 2) or geldanamycin (lanes 3 and 4) was applied. Immediately after the second drug addition, lysates were applied to luciferase immunoresins and further incubated for 20 min at 30 °C. After incubation, the immunoresins were washed three times with low-salt buffer before being subjected to a stringency wash either with low-salt buffer (L; odd-numbered lanes) or with high-salt buffer containing 0.5 M NaCl (H; even-numbered lanes). Washed immunoresins were eluted with SDS−PAGE sample buffer and analyzed by Western blotting with anti-hsp90 antibodies.

the finding that molybdate altered the k_{app} of luciferase renaturation machinery for ATP was consistent with our previous observation that inhibition of hsp90 function by geldanamycin similarly altered the k_{app} of the luciferase renaturation reaction for ATP (*10*). This finding indicated that molybdate's inhibition of luciferase renaturation was in some fashion related to the involvement of ATP in hsp90-mediated protein folding.

Effects of Free Phosphate on Luciferase Renaturation. It has previously been suggested that the mechanism of molybdate action is to serve as a transition state analogue of phosphate hydrolysis (for review, see ref *17*), thus prompting us to undertake a kinetic analysis of the effects of free phosphate (P_i) on luciferase renaturation. When varying fixed concentrations of P_i were added to dialyzed RRL which contained a saturating concentration of ATP and varying concentrations of luciferase, P_i was found to inhibit luciferase renaturation noncompetitively with respect to luciferase (Figure 4A). The replot of P_i concentration versus k_{app}/V_{app} appeared to be linear (not shown), yielding an estimated K_i for P_i of ~10 mM. The replot of P_i concentration versus $1/V_{app}$ was nonlinear (not shown), indicating that the binding of P_i molecules to the hsp90 chaperone machine exerted complex effects on luciferase renaturation.

Kinetic analysis of the effects of P_i on luciferase renaturation in dialyzed RRL also indicated that the binding of more than one molecule of ATP was involved in the mechanisn of luciferase renaturation facilitated by the hsp90 chaperone machine. When ATP concentrations were varied in the presence of a constant concentration of luciferase, addition of P_i to renaturation reaction mixtures yielded curved Eadie−Hofstee plots compared to the linear plots observed in the absence of P_i (Figure 4B). This effect of P_i on the shape of the kinetic plot was consistent with a model in which ATP bound twice during the reaction sequence, with an irreversible step (release of the product P_i) occurring between the two steps of ATP addition. According to this model, establishing a reversible connection between the two sites of ATP addition upon the addition of P_i to the reaction mixture would have caused the Eadie−Hofstee plot to become curved. The degree of curvature observed in the Eadie−Hofstee plots when the kinetic measurements were carried out in the presence of P_i suggested that there was a significant difference in the k_{app} values for the two binding sites for ATP.

Opposing Effects of Molybdate and Geldanamycin on the Affinity of Hsp90 for Its Substrates. The observation that molybdate inhibited the hsp90-dependent biogenesis of $p56^{lck}$-F505 by physically locking $p56^{lck}$F505 onto hsp90 machinery (Figure 1) prompted us to examine the effects of molybdate on physical interactions between hsp90 machinery and heat-denatured luciferase. For these assays, heat-denatured luciferase was immobilized to anti-luciferase immunoresins and subsequently incubated in RRL protein folding reaction mixtures. Although some hsp90 was recovered from control immunoresins lacking luciferase after the immunoresins were washed with low-ionic strength buffers, significantly more hsp90 was recovered from immunoresins to which denatured luciferase was bound (Figure 5A, lane 1 vs 3). This result confirmed our previous description (*10*) of physical associations between hsp90 and heat-denatured luciferase under these washing conditions. In contrast, the physical association of hsp90 with heat-denatured immobilized luciferase could not be detected following washing with buffer containing 0.5 M NaCl; under these conditions, the amount of hsp90 coadsorbed by anti-luciferase antibodies was reduced to that observed for control immunoresins lacking luciferase (Figure

5A, lane 4 vs 2). When molybdate was included in the RRL protein folding reaction mixtures and in buffers used to wash immunopellets, molybdate substantially increased the amount of hsp90 recovered from the luciferase immunoresins (Figure 5A, lane 9). Furthermore, molybdate stabilized the association of hsp90 with luciferase such that this association became stable to washing with buffer containing 0.5 M NaCl (Figure 5A, lane 10). These results demonstrated that the association of hsp90 machinery with luciferase behaved in a fashion similar to that previously described for steroid hormone receptors; the association was normally salt-labile but could be stabilized by molybdate.

The formation of molybdate-stabilized hsp90 complexes has been reported to be inhibited by the hsp90-binding drug geldanamycin (*16*, *23*, *47*). This observation prompted us to investigate the effects of geldanamycin on the molybdate-stabilized interaction between luciferase and hsp90. Although the normally salt-labile interaction of hsp90 with heat-denatured luciferase was rendered salt-resistant by molybdate (Figure 5A), addition of geldanamycin prior to molybdate prevented molybdate-induced salt resistance (Figure 5B). In contrast, when molybdate was added prior to geldanamycin, geldanamycin did not compromise molybdate-induced salt resistance (Figure 5B). Furthermore, the order of drug addition affected the nature of hsp90's association with luciferase in a manner that was not equivalent to simultaneous drug additions (not shown; see also ref *47*). These "order-of-addition" experiments demonstrated that molybdate and geldanamycin had opposing effects on the association of hsp90 with denatured luciferase.

In the absence of molybdate, hsp90 associates with its substrates luciferase, the progesterone receptor, and the glucocorticoid receptor in a salt-labile fashion (e.g., Figure 5A). In contrast to this salt-labile association, the association of hsp90 with p56^{lck} and with viral p60^{src} is stable to washing with very high-ionic strength buffers (up to 2 M NaCl), even when such complexes are prepared and analyzed in the absence of molybdate or related stabilizing agents (*28*, *48*). Although the biochemical basis for these differences in salt resistance is poorly understood, the salt resistance of the kinase·hsp90 heterocomplex provided an opportunity to examine the effects of geldanamycin on the nature of hsp90's association with p56^{lck}. Specifically, we hypothesized that geldanamycin might alter the mode by which hsp90 interacted with p56^{lck}. To test this hypothesis, we examined the effect of geldanamycin on the salt resistance of the hsp90·p56^{lck} complex. As previously shown (*26*−*28*), heterocomplexes containing hsp90 were co-immunoadsorbed by anti-p56^{lck} antibodies in a p56^{lck}-specific fashion (Figure 6). These complexes could be detected following washing under either low- or high-ionic strength conditions (Figure 6, lanes 2 and 3, respectively). The relative intensities of hsp90 bands thus observed suggested that the total hsp90 signal observed after low-salt washing was derived from a combination of salt-labile and salt-resistant contributions (cf. lanes 2 and 3). However, in translation reaction mixtures treated with 5 μg/mL geldanamycin, interactions between hsp90 and p56^{lck} were no longer detected following washing with 0.5 M NaCl (Figure 6, lane 5). Nonetheless, significant amounts of specific interaction between hsp90 and p56^{lck} could still be detected when hsp90·p56^{lck} complexes from geldanamycin-treated translations were washed in low-salt buffer (Figure 6, lane 4). Thus, geldanamycin disrupted the salt-stable interaction between hsp90 and p56^{lck}, but did not prevent the detection of weak salt-labile interactions between these proteins. This result supported the thesis hypothesis. Geldanamycin altered the mode by which hsp90 interacted with p56^{lck}.

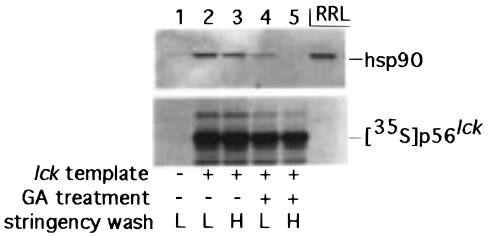

FIGURE 6: Effect of geldanamycin on the salt resistance of the hsp90·p56^{lck} heterocomplex. In vitro translation reactions were programmed for synthesis of p56^{lck} (lanes 2−5) in the presence of [^{35}S]Met and were supplemented with either Me_2SO_4 drug vehicle (lanes 1−3) or geldanamycin (lanes 4 and 5). A mock translation lacking template for p56^{lck} was also assessed (lane 1). After a brief protein synthesis, translation reaction mixtures were immunoadsorbed with anti-p56^{lck} antibodies. Each immunoadsorption mixture was washed three times in low-salt buffer, split into two equal aliquots, and subjected to a stringency wash with either low-salt buffer (L; lanes 1, 2, and 4) or high-salt buffer containing 0.5 M NaCl (H; lanes 3 and 5). After being washed, immunoresins were eluted with SDS−PAGE buffer and analyzed by Western blotting with anti-hsp90 antibodies to detect hsp90 coadsorbed as part of the hsp90·p56^{lck} heterocomplex (upper panel) or by autoradiography to assess immunoadsorption efficiency (lower panel). Also shown is the result with an aliquot of rabbit reticulocyte lysate applied to the gel as a standard for the detection of hsp90 (RRL).

To obtain further evidence that molybdate and geldanamycin enforced opposing structures upon hsp90, the ability of hsp90 to bind to immobilized geldanamycin was investigated in the presence and absence of molybdate pretreatments. As described previously by Whitesell et al. (*22*), hsp90 bound to immobilized geldanamycin in a specific (competable) fashion (Figure 7A, lane 1 vs 2). In contrast, pretreatment of the RRL reaction with 20 mM molybdate inhibited hsp90's subsequent ability to bind geldanamycin (Figure 7A, lane 3). These results indicated that under physiologic conditions, molybdate enforced hsp90 structures that were not able to bind to geldanamycin; this conclusion agreed nicely with the effects of the timing of dual drug applications on substrate interactions (Figure 5B).

Opposing Effects of Molybdate and Geldanamycin on Hsp90 Structure. To further investigate the biochemical phenomena underlying the effects of molybdate and geldanamycin, we utilized the monoclonal antibody AC88. Recognition of hsp90 by AC88 has been reported to require a poorly characterized epitope occurring within the last 149 C-terminal amino acids of the 728 residues that comprise chicken hsp90 (*30*). More precisely, residues 661−677 have been found to be required for recognition by AC88 (*31*). More importantly however, AC88 has been reported to have the unique property of immunoadsorbing free hsp90, but not hsp90 present in hsp90·substrate heterocomplexes (*29*). Since the effects of molybdate on substrate association suggested that treatment with molybdate traps hsp90 in a structure that interacts tightly with substrates, we hypothesized that molybdate might alter hsp90's structure in a similar fashion even when no substrate was added. We found that while 2.0 μg of AC88 could nearly quantitatively subtract the hsp90

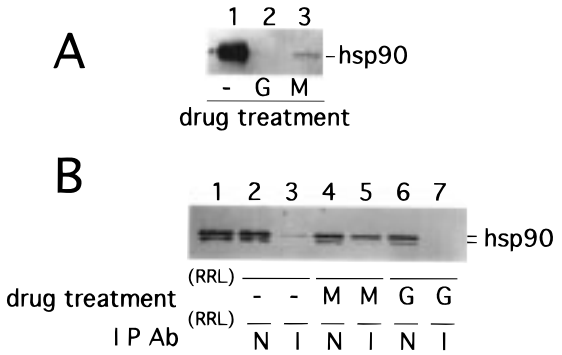

FIGURE 7: Effects of molybdate on hsp90. (A) Rabbit reticulocyte lysate reaction mixtures containing an ATP-regenerating system were preincubated for 5 min at 37 °C in the absence of drug (lane 1), in the presence of soluble geldanamycin (lane 2), or in the presence of molybdate (lane 3) and were subsequently incubated with geldanamycin affinity resin (geldanamycin covalently coupled to Affigel beads). After binding, geldanamycin resins were washed, bound materials were eluted by boiling in SDS−PAGE sample buffer, and eluted materials were analyzed by Western blotting with anti-hsp90 antibodies. (B) Rabbit reticulocyte reaction mixtures containing an ATP-regenerating system were preincubated in the absence of drug (lanes 2 and 3), in the presence of molybdate (M; lanes 4 and 5), or in the presence of geldanamycin (G; lanes 6 and 7). After preincubation, 2.0 μL aliquots from each reaction mixture were immunoadsorbed with either nonimmune antibody (N; lanes 2, 4, and 6) or AC88 monoclonal anti-hsp90 antibody (I; lanes 3, 5, and 7). After immunoadsorption, the supernatant fractions containing unadsorbed proteins were collected and analyzed by SDS−PAGE and Western blotting with anti-hsp90. Additionally, an aliquot of RRL was applied to the gel as a standard for the detection of hsp90 (RRL; lane 1).

population from 2.0 μL of untreated RRL reaction mixture, treatment of RRL reaction mixtures with 20 mM molybdate caused approximately 45% of the hsp90 in these reaction mixtures to be unrecognizable to AC88 (Figure 7B). Thus, even in the absence of exogenous hsp90 substrate, molybdate induced hsp90 structures that resembled those assumed when hsp90 bound tightly to its substrates.

To further identify regions of hsp90 that might be affected during molybdate-induced structural trapping, we utilized mild proteolytic nicking in conjunction with Western blotting with antibodies against each terminus of hsp90. We chose this approach rather than using purified chaperone preparations to acknowledge the potential contributions of hsp90's partner proteins. Results from these studies are presented as Western blots in Figure 8 and graphically in Figure 9.

To map regions of tryptic cleavage of hsp90, we compared our digestion products to those previously reported by Nemoto et al. (*49*). These authors observed five regions at which trypsin cleaved purified hsp90 and identified two specific cut sites by sequencing trypsinolysis products. These authors observed that ready cleavage at a region 401 residues from the N-terminus of recombinant human hsp90α yielded a major 50 kDa N-terminal fragment. Similarly, ready cleavage 616 and 621 residues from the N-terminus yielded a major 80 kDa N-terminal fragment. Additionally, Nemoto et al. observed that less frequent cleavage at two additional sites produced N-terminal fragments of approximately 40 and 32 or 33 kDa; however, the precise residues corresponding to these latter cut sites were not identified.

We observed that trypsinolysis of hsp90 present in ATP-replete RRL yielded a pattern of N-terminal fragments (Figure 8A) corresponding closely to that observed by

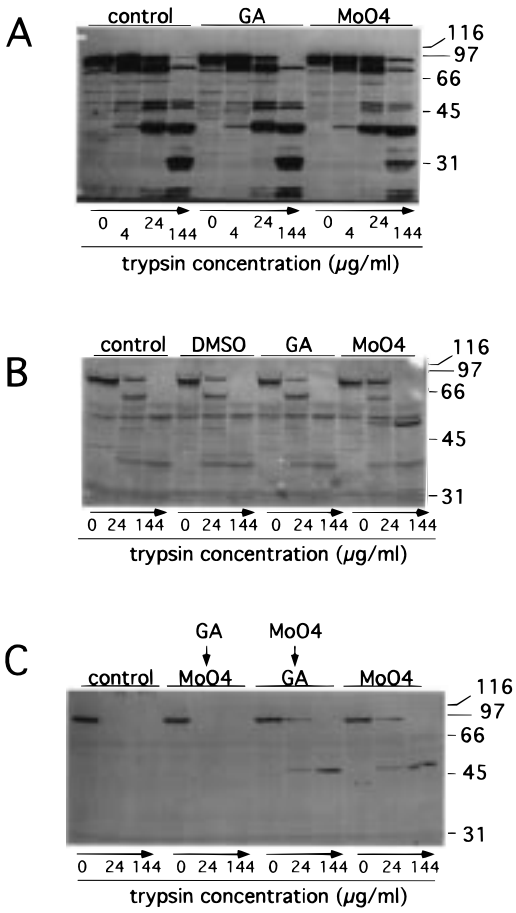

FIGURE 8: Proteolytic mapping of altered hsp90 structure induced by molybdate. (A and B) Rabbit reticulocyte lysate reaction mixtures containing an ATP-regenerating system were incubated for 5 min at 37 °C in the absence of drug (control), in the presence of geldanamycin (GA), or in the presence of molybdate (MoO4). After drug treatment, reaction mixtures were chilled and incubated on ice with the indicated concentrations of trypsin. Trypsinolyzed reaction mixtures were boiled in SDS−PAGE buffer and analyzed by SDS−PAGE and Western blotting with antibodies directed against the N-terminus (A) or against the C-terminus (B) of hsp90. Migrations and molecular masses of size standards are indicated along the right side of each panel. (C) The effects of sequential applications of geldanamycin and molybdate were assessed; additionally, the effects of single drug additions were assessed as controls. For sequential additions, lysates were preincubated for 5 min at 37 °C with either geldanamycin or molybdate, after which the second drug, either molybdate or geldanamycin, was applied (GA → MoO4 and MoO4 → GA, respectively). Reaction mixtures were then further incubated for 5 min at 37 °C, chilled and trypsinolyzed, and assessed by SDS−PAGE and Western blotting with antibodies directed against the C-terminus of hsp90.

Nemoto et al. (*49*). In untreated ATP-replete RRL, mild trypsinolysis produced two major hsp90 fragments that could be detected by antibodies recognizing the N-terminus, one with an M_r of approximately 78 000 and one with an M_r of approximately 40 000. Additionally, we detected five minor fragments containing the hsp90 N-terminus; these fragments migrated with M_r values of 51 000, 48 000, 30 000, 24 000, and 22 000.

When we compared our proteolysis patterns generated in RRL with those documented by Nemoto et al. for purified hsp90 (*49*), one significant difference was noted regarding the relative abundance of the 40 and 50 kDa fragments observed in each study. For purified hsp90, Nemoto et al. observed that a 50 kDa N-terminal fragment appeared at

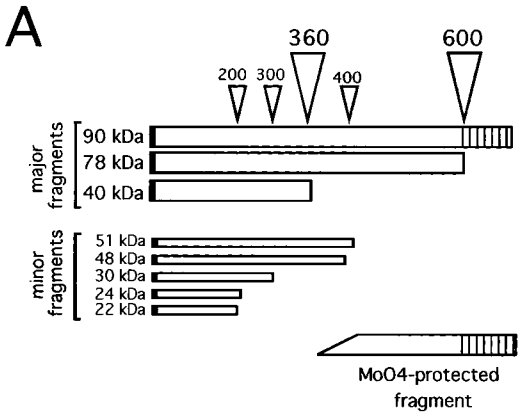

B

G_{605}WTANMERIMKAQALRDNSTMG_{626}

(Region 600)

FIGURE 9: Hsp90 proteolytic map. (A) Full-length hsp90 and its N-terminal fragments generated by trypsinolysis are represented as proportional rectangles, with their approximate molecular masses indicated in kilodaltons. The approximate positions of the N-terminal (black boxes) and C-terminal epitopes (vertical hatching) are indicated. Deduced sites of proteolytic cutting are indicated by inverted triangles, with each down-pointing vertex indicating the relative position of cleavage on full-length hsp90, and the number above each triangle indicating the numerical designation for each region. Large triangles represent relatively susceptible sites of cleavage that generate predominant N-terminal fragments, while smaller triangles represent relatively resistant sites of cleavage that generate minor N-terminal fragments. The upward-slanting N-terminus of the MoO4-protected fragment indicates uncertainty regarding the site of cleavage that generates this fragment. (B) The human hsp90 amino acid sequence from residue 605 to 626 is shown with an arbitrary delineation at glycines based on the speculation that these residues confer flexibility. Residues are numbered as they are for human hsp86, and those residues immediately N-terminal of trypsinolysis sites identified by Nemoto et al. (*49*) are underlined.

relatively low trypsin concentrations, followed by subsequent appearance of a 40 kDa N-terminal fragment at higher trypsin concentrations. In contrast, we observed that trypsinolysis of hsp90 present in ATP-replete RRL produced the 40 kDa fragment as one of the two major proteolysis products, while 50 kDa fragments (M_r values of 51 000 and 48 000) were minor products relative to the 40 kDa fragment.

Other than this difference in the relative abundance of these two fragments, the cleavage patterns and the M_r values of hsp90 fragments produced in RRL (Figure 9) indicated that hsp90 present in ATP-replete RRL was susceptible to mild proteolytic nicking at regions previously found to be the major and minor sites cleaved during mild proteolytic nicking of purified hsp90 (*49*). Thus, the 78 kDa fragment that we observed likely corresponded to the 80 kDa fragment reported by Nemoto et al. (*49*) and thus resulted from cleavage at residues occurring approximately 600 amino acids from the N-terminus (subsequently denoted Region 600). Similarly, the minor 50 kDa doublet we observed likely corresponded to cleavage at residues occurring approximately 400 amino acids from the N-terminus (subsequently denoted Region 400). Furthermore, although Nemoto et al. did not precisely identify the residues that were cleaved to yield their 40 kDa fragment, we calculate that our major 40 kDa fragment results from proteolysis of a relatively susceptible site lying approximately 360 residues from the N-terminus (subsequently denoted Region 360) while the 34, 24, and 22 kDa fragments are calculated to result from proteolysis of relatively resistant sites lying approximately 300 residues (34 kDa fragment) and 200 residues (24 and 22 kDa fragments) from the N-terminus (subsequently referred to as Regions 300 and 200, respectively). Thus, our data indicated that hsp90 present in ATP-replete RRL contained two regions of major susceptibility to proteolysis (one mapping to Region 600 and one mapping to Region 360) and three additional regions with lower sensitivities to proteolysis (Regions 400, 300, and 200). This proteolytic map is presented graphically in Figure 9.

Having established a proteolytic map for hsp90 present in untreated ATP-replete RRL, we assessed the effects of geldanamycin and molybdate on the hsp90 proteolytic fingerprint. This was accomplished by incubating ATP-replete RRL reaction mixtures with these agents for 5 min at 37 °C prior to chilling and proteolytic nicking. Geldanamycin had no discernible effect on the hsp90 fingerprint (Figure 8A), a finding consistent with the recent suggestion that the geldanamycin-bound conformation of hsp90 resembles its default state (*25*). Nor did modification of nucleotide ratios (treatment with apyrase and/or exogenously added ADP) or oxidizing agents (NEM, diamide, and peroxide) affect hsp90's proteolytic fingerprint (not shown). Furthermore, the nucleotide mimetics sodium fluoride and P_i did not affect hsp90's proteolytic fingerprint (not shown).

In contrast, treatment of RRL reaction mixtures with 20 mM molybdate significantly stabilized full-length hsp90 against proteolysis (Figure 8A). This protection was accompanied by a small decrease in the detection of the 48 kDa trypsinolytic fragment produced by proteolysis in Region 400. These results were evident only when molybdate was added directly to RRL reaction mixtures; addition of molybdate directly to trypsin prior to fingerprinting did not similarly alter hsp90's fingerprint (not shown). Thus, molybdate treatment generated a specific form of hsp90 or hsp90 machinery with an altered sensitivity to trypsin.

Although molybdate treatment resulted in a decrease in the signal from the 48 kDa N-terminal fragment concomitant with protection of full-length hsp90, the magnitude of this decrease did not appear to be sufficient to explain the corresponding increase in the amount of full-length hsp90 detected (Figure 8A). To identify other cleavage sites in hsp90 whose resistance to cleavage may have been induced by molybdate, hsp90 fragments containing the C-terminus were detected by Western blotting with the AC88 monoclonal antibody (Figure 8B). Although Western blots created with AC88 were much less sensitive than those created with polyclonal antisera and required analysis of larger aliquots of RRL, such blots confirmed that full-length hsp90 experienced a significant degree of protection from proteolysis in molybdate-treated RRL. More importantly, proteolysis of molybdate-treated RRL resulted in a single novel C-terminal hsp90 fragment migrating at 50 kDa that was not observed in untreated RRL or in RRL treated with geldanamycin. The size of this fragment (M_r of approximately 50 000 ± 1300) in conjunction with the presence of the AC88 epitope suggested that its N-terminus mapped to a region ap-

proximately 450 residues from the C-terminus. Thus, the N-terminus of this fragment probably occurred at Region 400, but difficulties inherent to the study of hsp90 in whole RRL prevented us from ruling out Region 360 as the potential N-terminus of this fragment. Most importantly, however, the appearance of this molybdate-protected C-terminal fragment, in conjunction with its size, indicated that hsp90 incubated in the presence of molybdate experienced dramatic protection from proteolysis within Region 600, despite the fact that this region is normally very vulnerable in untreated lysates. This conclusion was consistent with the reproducible observation that the degree of protection of full-length hsp90 by molybdate was reproducibly correlated with a decrease in the signal from the 78 kDa N-terminal fragment (not shown); however, this result was not apparent for the heavily developed immunoblot shown in Figure 8B.

To test the hypothesis that molybdate's protection of hsp90 against proteolysis might be unrelated to the effects of molybdate on substrate affinity, we again performed sequential order-of-addition experiments utilizing molybdate and geldanamycin. We hypothesized that molybdate might protect hsp90 from proteolysis irrespective of the presence and/or timing of geldanamycin addition, and thus might demonstrate that there was not a relationship between molybdate-enforced substrate affinity and molybdate-enforced resistance to proteolysis. Instead, we found that the molybdate did not protect hsp90 against proteolysis when geldanamycin was applied prior to molybdate treatment (Figure 8C). Similarly, treatment with geldanamycin after molybdate treatment did not abrogate the molybdate-induced protection of Region 600 of hsp90 (Figure 8C). The results indicated that, as was observed for the effects of these drugs on substrate interactions, geldanamycin and molybdate affected hsp90's proteolytic fingerprint in opposing fashions.

DISCUSSION

Molybdate and Geldanamycin Alter the Mode by Which Hsp90 Interacts with Substrates and Inhibit Hsp90-Dependent Processes. Data presented in this report and elsewhere indicate that hsp90 has at least two different modes by which it can interact with substrates. For the hsp90-dependent kinases $p56^{lck}$ and viral $p60^{src}$, a molybdate-independent salt-stable interaction between hsp90 and kinase folding intermediates accompanies kinase biogenesis (Figure 6). Additionally, the total population of hsp90·$p56^{lck}$ heterocomplexes may also include a salt-labile subpopulation (Figure 6). In contrast to the $p56^{lck}$·hsp90 heterocomplex, interactions between hsp90 and steroid hormone receptors are not normally stable in the presence of moderate to high concentrations of salt; however, receptor·hsp90 heterocomplexes become salt-resistant when analyzed in the presence of molybdate (for review, see ref *17*). For a third class of hsp90 substrates, heat-denatured firefly luciferase, renaturation is accompanied by a physical association with hsp90 that is salt-sensitive, but can be stabilized by molybdate to become salt-resistant (Figure 5A). Thus, heat-denatured luciferase associates with hsp90 in a fashion that is analogous to that of reconstituted receptor·hsp90 heterocomplexes and that differs from that of heterocomplexes formed between hsp90 and newly synthesized kinase molecules. In addition to this similarity, luciferase·hsp90 heterocomplexes have a composition of hsp90 cohorts that is to date indistinguishable from that of receptor·hsp90 heterocomplexes (*10*).

The hsp90 inhibitor geldanamycin alters the mode by which hsp90 interacts with $p56^{lck}$. Although $p56^{lck}$ biogenesis is normally accompanied by a salt-resistant association with hsp90, $p56^{lck}$ molecules synthesized in the presence of geldanamycin subsequently associate with hsp90 only in a salt-labile fashion (Figure 6). This finding suggests that discrepancies in the literature regarding the effects of geldanamycin on hsp90·substrate complexes (*39*, *50*) may reflect differences in the ionic strengths of buffers used to lyse cells and wash immunocomplexes. This observation also provides significant insight into the biochemistry of hsp90 machinery and the effects of geldanamycin on hsp90 function (discussed below).

Like geldanamycin, molybdate alters the mode by which hsp90 interacts with its substrates. Molybdate has been utilized for years to stabilize the hormone-binding competence of receptor·hsp90 heterocomplexes (for review, see ref *17*). Subsequently, descriptions of the stabilizing effect of molybdate on hsp90·protein heterocomplexes have been expanded to include a diverse group of hsp90 substrates, indicating that molybdate acts directly on hsp90 machinery rather than on the hsp90 substrate per se (*45*). This supposition is supported by the recent demonstration that molybdate directly stabilizes the interaction of hsp90 with its p23 cohort (*15*, *16*). Consistent with these previous findings, we find that molybdate enforces the association of hsp90 with its substrates $p56^{lck}$ and heat-denatured luciferase (Figures 1A and 5A).

Thus, both molybdate and geldanamycin alter the mode by which hsp90 interacts with its substrates, enforcing hsp90 structures with high and low affinities for substrates, respectively. Furthermore, order-of-addition experiments indicate that these compounds have opposing effects on hsp90−substrate interactions; prior treatment of RRL with either compound abolishes the effects of the other (Figure 5). This opposing relationship is consistent with previous work in which the effects of these compounds on the association of hsp90 with progesterone receptors were examined (*47*) and is consistent with the results presented here regarding the opposing effects of these compounds on hsp90 structure (Figures 7B and 8) and the effect of molybdate on hsp90's ability to bind geldanamycin resin (Figure 7A). In addition to enforcing (or forbidding) alternative modes of hsp90−substrate interactions, geldanamycin (*10*, *27*) and molybdate (Figures 1 and 2) also inhibit the hsp90-mediated processes of $p56^{lck}$ biogenesis and luciferase renaturation. These observations suggest that the ability of hsp90 to cycle between two alternative modes of interaction is a requisite for hsp90 function, since neither mode of association with folding substrates is in itself sufficient to produce active luciferase or $p56^{lck}$ molecules. This conclusion is consistent with the previous demonstration that hsp90 machinery interacts with progesterone receptors in a dynamic, rather than static, fashion (*51*).

In addition to demonstrating that molybdate inhibits hsp90-mediated protein folding, kinetic analyses of luciferase renaturation in molybdate-treated RRL provide other insights into chaperone-mediated renaturation of proteins. Although molybdate can inhibit luciferase renaturation nearly completely at limiting luciferase concentrations (Figure 2A), at

saturating luciferase concentrations molybdate is much less effective (Figure 2B). However, the fraction of the saturating luciferase population that renatures despite high molybdate concentrations does not represent passive chaperone-independent renaturation, because renaturation of luciferase at significant rates in RRL requires ATP (*8*−*10*), indicating the involvement of an active (chaperone) principle. Thus, molybdate does not globally inhibit all chaperone activities in RRL, but is instead specific for hsp90-mediated folding processes. These observations support the previously postulated existence of two alternative pathways for luciferase renaturation in RRL: an efficient hsp90-mediated pathway that can be inhibited by geldanamycin and a kinetically slow pathway that is geldanamycin-resistant (*10*). This interpretation argues that the kinetically faster hsp90-dependent pathway is the preferred pathway for protein renaturation at limiting denatured substrate concentrations. However, when hsp90 function is inhibited, renaturation may proceed through the alternative kinetically slower hsc70-dependent/hsp90-independent pathway. This interpretation argues that at limiting luciferase concentrations, luciferase molecules become trapped on the molybdate-poisoned hsp90 pathway. This postulation of two alternative pathways for luciferase renaturation is consistent with in vitro renaturation experiments in which purified components are used, wherein luciferase can be renatured in the presence of hsc70 and HDJ-2/YDJ-1 alone, but can renature more efficiently when hsp90 and p60HOP are also present (*52*).

In addition to illuminating molybdate's role as an inhibitor of hsp90, kinetic analyses also provide hints about the potential nature of the alternative renaturation pathway and its relationship to the hsp90-dependent pathway. Both hsp90 and hsc70 are physically and functionally involved in the process of luciferase renaturation (*10*, *52*−*56*), thus implying two sites of addition of ATP in this process (the nucleotide binding pocket of hsc70 and the nucleotide binding pocket of hsp90). The presumed existence of more than one site of ATP addition predicts that Eadie−Hofstee plots of rate of luciferase renaturation versus ATP concentration should yield curved lines. However, such plots are clearly and reproducibly linear (Figure 3 and ref *10*). This result suggests that an irreversible step, such as product release, occurs between the two ATP addition events. Such a two-site model is supported by the observation that addition of P_i to RRL folding reaction mixtures produces the predicted curved Eadie−Hofstee plots of ATP concentration versus rate of renaturation (Figure 4). This effect is consistent with a model in which luciferase renaturation proceeds through a pathway(s) involving two sites for addition of ATP, with ATP hydrolysis and release of P_i occurring prior to the addition of the second ATP molecule (i.e., curved Eadie−Hofstee plots are observed if a reversible connection between the two ATP sites is established by the addition of high levels of the product P_i to dialyzed RRL). Furthermore, the effect of high levels of phosphate on the kinetic plots indicates that release of phosphate from hsp90 or hsc70 chaperone machinery is a mechanistic step in the folding process that occurs between the two postulated ATP addition events and further prompts us to speculate that phosphate release may regulate communication between the two ATP-binding sites and their corresponding chaperone(s).

Additionally, for this two-site model, the ratio of the slopes of the asymptopes to the two extremes of the curve is roughly proportional to the ratio of the k_{app} values for the two ATP sites. Estimates of these slopes suggest that the k_{app} values for the two sites differ by at least 50-fold. The low and high k_{app} sites thus described may represent the binding of ATP to hsc70 and hsp90, respectively, a speculation that is consistent with the relative affinities of these chaperones for ATP. However, the high-k_{app} site for ATP is not apparent when the rate of luciferase renaturation was determined in the presence of moybdate and varying ATP concentrations (Figure 3). This finding suggests that molybdate specifically affects only the high-k_{app} ATP site and inhibits the preferred hsp90-dependent luciferase renaturation pathway, but allows luciferase to renature through the kinetically slower alternative hsc70-dependent pathway.

Inhibition of Hsp90 by Molybdate Produces Hsp90 Molecules with Altered Structure. This altered structure is apparent as a dramatic molybdate-induced protection against proteolysis mapping to Region 600 of hsp90, with a less dramatic protection apparent in Region 400 (Figures 8 and 9). The precise C-terminal site of proteolysis protected very likely corresponds to the C-terminal trypsinolysis site previously mapped to amino acids 616 and 621 by Nemoto et al. (*49*). This region of hsp90 is highly conserved, and 3 of 19 point mutations known to alter hsp90 function occur within this region (*40*, *57*−*59*). Additionally, deletion of residues 601−620 or residues 381−441 from chicken hsp90 abolishes its ability to bind to the progesterone receptor; these regions correspond to Regions 600 and 400, respectively, identified in our work presented here (cf. Figures 8 and 9 and ref *30*). Additionally, analysis of recombinant constructs or chymotryptic fragments has implicated residues 542−732 of human hsp90α as an important determinant of hsp90 dimerization (*60*). Furthermore, the isolated C-terminal domain of hsp90 prevents protein aggregation and binds peptides (*61*, *62*). [Although similar antiaggregation activity has also been reported for the N-terminal domain of hsp90 (*61*, *62*), our current results do not allow us to discriminate between putative substrate binding domains of hsp90.] Additionally, it has been demonstrated that the C-terminal domain of hsp90 is recognized by the TPR domains of immunophilins and p60HOP (*63*). On the basis of the opposing effects of geldanamycin and molybdate on hsp90−substrate interactions and on molybdate's protection of hsp90 from proteolysis at a site likely occurring at amino acids 616 and 621, we conclude that Region 600 of hsp90 functions in some fashion to mediate hsp90's interaction with substrates. Ready cleavage of this region in the absence of molybdate indicates that this motif is normally very flexible and unstructured, suggesting that it may serve as a hinge (*60*) or similar dynamic structure. Molybdate-induced protection from proteolysis may thus result from direct restructuring of this motif by conformational switching, or might result from masking of this region by direct binding to p23, immunophilins, and/or substrate. Additionally, molybdate's subtle protective effect at other sites of proteolysis argues that molybdate may induce additional less dramatic (relative to Region 600) global or allosteric alterations in hsp90's conformation.

While we have not examined cohort composition in this study, previous work by others (*16*, *23*) indicates that structural locking of hsp90 by geldanamycin and molybdate

is accompanied by changes in cohort composition. Geldanamycin inhibits the formation of hormone receptor heterocomplexes containing hsp90, p23, and immunophilins ("late" receptor heterocomplexes) and causes an accumulation of receptor heterocomplexes containing hsp90, p60HOP, and hsp70 ("intermediate" heterocomplexes). In contrast to geldanamycin, molybdate stabilizes the normally salt-labile interaction of receptors with hsp90, p23, and immunophilins, but does not lead to an accumulation of salt-resistant receptor heterocomplexes containing hsp90, p60HOP, and hsp70 (*47*). [However, under low-salt conditions, molybdate enhances the stability of intermediate heterocomplexes (*14*).] Thus, these previously documented effects of geldanamycin and molybdate on cohort compositions correlate with findings presented here that these compounds alter hsp90 structure and the mode by which hsp90 interacts with its substrates. This conclusion is consistent with a previous study in which the effects of geldanamycin and molybdate on the salt resistance of progesterone receptor heterocomplexes were examined, from which it was concluded that each of these two hsp90 machineries (late and intermediate) interacts with the progesterone receptor in distinct fashions (*47*). Correlations between the opposing effects of geldanamycin and molybdate on hsp90's cohort compositions, its protease resistance, and its mode of binding to substrates suggest a relationship between these three aspects of hsp90 structure and function. However, work to date does not allow us to elucidate cause-and-effect relationships among these three aspects.

Our results contribute to evolving models for hsp90 function which postulate that nucleotide binding, hydrolysis, and exchange mediate switching of hsp90 between alternative conformations (*15*, *19*, *24*, *62*). We speculate that the molybdate-locked form of hsp90 represents a slow-off, slow-on closed chaperone conformation by which hsp90 binds directly to its substrates via hydrophobic interactions. In contrast, the geldanamycin-bound form of hsp90 would represent a fast-off, fast-on open conformation of hsp90 with a weak affinity for substrate; this low-affinity geldanamycin-locked conformation of hsp90 may not associate with its substrates per se, but instead may be electrostatically associated with cohort proteins (e.g., hsp70 and p60HOP) which are directly bound to substrate. These alternative modes by which hsp90 can interact with substrates may reflect portions of an hsp90 reaction cycle similar to those previously observed for GroEL and DnaK. Alternatively, the primary effects of molybdate and geldanamycin may be to enforce specific hsp90 cohort compositions, and the effects of these compounds on hsp90−substrate interactions may simply reflect specific enforced interactions of hsp90 with substrate-bound cohorts.

In summary, we find that molybdate and geldanamycin have opposing inhibitory effects on hsp90, enforcing hsp90 structures with high and low affinities for substrates, respectively. These effects accompany altered hsp90 structure, particularly at its C-terminus, suggesting that this region of hsp90 is a primary determinant of the nature by which hsp90 interacts with substrate.

NOTE ADDED DURING REVISION

A recent study by Soti et al. (*64*) demonstrates that permolybdate binds to purified hsp90 and induces changes in the electrophoretic mobility of the full-length protein and its tryptic fragments.

ACKNOWLEDGMENT

Geldanamycin was provided by the Drug Synthesis and Chemistry Branch, Developmental Therapeutics Program, Division of Cancer Treatment, National Cancer Institute. DNA sequencing was performed by the Oklahoma State University Recombinant DNA/Protein Resource Facility. Polyclonal ascites fluid was produced by the Oklahoma State University Hybridoma Center for the Agricultural and Biological Sciences. We thank Drs. Richard Essenberg and H. Olin Spivey (Oklahoma State University) for their assistance in interpretion of kinetic data and Dr. Uma Sheri (Oklahoma State University) for insightful discussions and for critical reading of the manuscript. Additionally, we thank Dr. R. Pearlmutter (Howard Hughes Medical Institute, University of Washington, Seattle, WA) for providing plasmid DNAs encoding wild-type and F505 forms of $p56^{lck}$.

REFERENCES

1. Ellis, R. J. (1993) *Philos. Trans. R. Soc. London, Ser. B 339*, 257−261.
2. Hartl, F. U. (1995) *Philos. Trans. R. Soc. London, Ser. B 348*, 107−112.
3. Gething, M.-J., and Sambrook, J. (1992) *Nature 355*, 33−45.
4. Hartl, F. U. (1996) *Nature 381*, 571−580.
5. Fenton, W. A., and Horwich, A. L. (1997) *Protein Sci. 6*, 743−760.
6. Bakau, B., and Horwich, A. L. (1998) *Cell 92*, 351−366.
7. Smith, D. F., Stensgard, D. B., Welch, W. J., and Toft, D. O. (1992) *J. Biol. Chem. 267*, 1350−1356.
8. Nimmesgern, E., and Hartl, F. U. (1993) *FEBS Lett. 331*, 25−30.
9. Schumacher, R. J., Hurst, R., Sullivan, W. P., McMahon, N. J., Toft, D. O., and Matts, R. L. (1994) *J. Biol. Chem. 269*, 9493−9499.
10. Thulasiraman, V., and Matts, R. L. (1996) *Biochemistry 35*, 13443−13450.
11. Johnson, J. L., and Toft, D. O. (1994) *J. Biol. Chem. 269*, 24989−24993.
12. Johnson, J. L., Corbisier, R., Stensgard, B., and Toft, D. O. (1996) *J. Steroid Biochem. Mol. Biol. 56*, 31−37.
13. Owens-Grillo, J. K., Stancato, L. F., Hoffmann, K., Pratt, W. B., and Krishna, P. (1996) *Biochemistry 35*, 15249−15255.
14. Dittmar, K. D., Demady, D. R., Stancato, L. F., Krishna, P., and Pratt, W. B. (1997) *J. Biol. Chem. 272*, 21213−21220.
15. Sullivan, W., Stensgard, B., Caucutt, G., Bartha, B., McMahon, N., Alnemri, E. S., Litwack, G., and Toft, D. (1997) *J. Biol. Chem. 272*, 8007−8012.
16. Johnson, J. L., and Toft, D. O. (1995) *Mol. Endocrinol. 9*, 670−678.
17. Pratt, W. B., and Toft, D. O. (1997) *Endocr. Rev. 18*, 306−360.
18. Prodromou, C., Roe, S. M., O'Brien, R., Ladbury, J. E., Piper, P. W., and Pearl, L. H. (1997) *Cell 90*, 65−75.
19. Grenert, J. P., Sullivan, W. P., Fadden, P., Haystead, T. A. J., Clark, J., Mimnaugh, E., Krutzsch, H., Oche, H.-J., Schulte, T. W., Sausville, E., Neckers, L. M., and Toft, D. O. (1997) *J. Biol. Chem. 272*, 23843−23850.
20. Scheibel, T., Neuhofen, S., Weikl, T., Mayr, C., Reinstein, J., Vogel, P. D., and Buchner, J. (1997) *J. Biol. Chem. 272*, 18608−18613.
21. Stebbins, C. E., Russo, A. A., Schneider, C., Rosen, N., Hartl, F. U., and Pavietich, N. P. (1997) *Cell 89*, 239−250.
22. Whitesell, L., Mimnaugh, E. G., De Costa, B., Myers, C. E., and Neckers, L. M. (1994) *Proc. Natl. Acad. Sci. U.S.A. 91*, 8324−8328.

23. Smith, D. F., Whitesell, L., Nair, S. C., Chen, S., Prapapanich, V., and Rimerman, R. A. (1995) *Mol. Cell. Biol. 15*, 6804−6812.
24. Csermely, P., Kajtar, J., Hollosi, M., Jalsovszky, J., Holly, S., Kahn, C. R., Gergely, P., Jr., Soti, C., Mihaly, K., and Somogyi, J. (1993) *J. Biol. Chem. 268*, 1901−1907.
25. Toft, D. O. (1998) *Trends Endocrinol. Metab. 9*, 238−243.
26. Hartson, S. D., and Matts, R. L. (1994) *Biochemistry 33*, 8912−8920.
27. Hartson, S. D., Barrett, D. J., Burn, P., and Matts, R. L. (1996) *Biochemistry 35*, 13451−13459.
28. Hartson, S. D., Ottinger, E. A., Huang, W., Barany, G., Burn, P., and Matts, R. L. (1998) *J. Biol. Chem. 273*, 8475−8482.
29. Riehl, R. M., Sullivan, W. P., Vroman, B. T., Bauer, V. J., Pearson, G. R., and Toft, D. O. (1985) *Biochemistry 24*, 6586−6591.
30. Sullivan, W. P., and Toft, D. O. (1993) *J. Biol. Chem. 268*, 20373−20379.
31. Chen, H.-S., Singh, S. S., and Perdew, G. H. (1997) *Arch. Biochem. Biophys. 348*, 190−198.
32. Ullrich, S. J., Robinson, E. A., Law, L. W., Willingham, M., and Appella, E. (1986) *Proc. Natl. Acad. Sci. U.S.A. 83*, 3121−3125.
33. Danielian, S., Fagard, R., Alcover, A., Acuto, O., and Fischer, S. (1989) *Eur. J. Immunol. 19*, 2183−2189.
34. Matts, R. L., Xu, Z., Pal, J. K., and Chen, J.-J. (1992) *J. Biol. Chem. 267*, 18160−18167.
35. Bohen, S. P., Kralli, A., and Yamamoto, K. R. (1995) *Science 268*, 1303−1304.
36. Xu, Y., and Lindquist, S. (1993) *Proc. Natl. Acad. Sci. U.S.A. 90*, 7074−7078.
37. Stancato, L. F., Chow, Y.-H., Hutchison, K. A., Perdew, G. H., Jove, R., and Pratt, W. B. (1993) *J. Biol. Chem. 268*, 21711−21716.
38. Wartmann, M., and Davis, R. J. (1994) *J. Biol. Chem. 269*, 6695−6701.
39. Schulte, T. W., Blagosklonny, M. V., Ingui, C., and Neckers, L. (1995) *J. Biol. Chem. 270*, 24585−24588.
40. Van Der Straten, A., Rommel, C., Dickson, B., and Hafen, E. (1997) *EMBO J. 16*, 1961−1969.
41. Matts, R. L., and Hurst, R. (1989) *J. Biol. Chem. 264*, 15542−15547.
42. Uma, S., Hartson, S. D., Chen, J.-J., and Matts, R. L. (1997) *J. Biol. Chem. 272*, 11648−11656.
43. Courtneidge, S. A., and Bishop, J. M. (1982) *Proc. Natl. Acad. Sci. U.S.A. 79*, 7117−7121.
44. Brugge, J., Yonemoto, W., and Darrow, D. (1983) *Mol. Cell. Biol. 3*, 9−19.
45. Hutchison, K. A., Stancato, L. F., Jove, R., and Pratt, W. B. (1992) *J. Biol. Chem. 267*, 13952−13957.
46. Marth, J. D., Cooper, J. A., King, C. S., Ziegler, S. F., Tinker, D. A., Overell, R. W., Krebs, E. G., and Perlmutter, R. M. (1988) *Mol. Cell. Biol. 8*, 540−550.
47. Chen, S., Prapapanich, V., Rimerman, R. A., Honore, B., and Smith, D. F. (1996) *Mol. Endocrinol. 10*, 682−693.
48. Brugge, J. S. (1986) *Curr. Top. Microbiol. Immunol. 123*, 1−22.
49. Nemoto, T., Sato, N., Iwanari, H., Yamashita, H., and Takagi, T. (1997) *J. Biol. Chem. 272*, 26179−26187.
50. Stancato, L. F., Silverstein, A. M., Owens-Grillo, J. K., Chow, Y.-H., Jove, R., and Pratt, W. B. (1997) *J. Biol. Chem. 272*, 4013−4020.
51. Smith, D. (1993) *Mol. Endocrinol. 7*, 1418−1429.
52. Johnson, B. D., Schumacher, R. J., Ross, E. D., and Toft, D. O. (1998) *J. Biol. Chem. 273*, 3679−3686.
53. Yonehara, M., Minami, Y., Kawata, Y., Nagai, J., and Yahara, I. (1996) *J. Biol. Chem. 271*, 2641−2645.
54. Schumacher, R. J., Hansen, W. J., Freeman, B. C., Alnemri, E., Litwack, G., and Toft, D. O. (1996) *Biochemistry 35*, 14889−14898.
55. Schneider, C., Sepp-Lorenzino, L., Nimmesgern, E., Ouerfelli, O., Danishefsky, S., Rosen, N., and Hartl, F. U. (1996) *Proc. Natl. Acad. Sci. U.S.A. 93*, 14536−14541.
56. Forreiter, C., Kirschner, M., and Nover, L. (1997) *Plant Cell 9*, 2171−2181.
57. Bohen, S. P., and Yamamoto, K. R. (1993) *Proc. Natl. Acad. Sci. U.S.A. 90*, 11424−11428.
58. Cutforth, T., and Rubin, G. M. (1994) *Cell 77*, 1027−1036.
59. Nathan, D. F., and Lindquist, S. (1995) *Mol. Cell. Biol. 15*, 3917−3925.
60. Nemoto, T., Ohara-Nemoto, Y., Ota, M., Takagi, T., and Yokoyama, K. (1995) *Eur. J. Biochem. 233*, 1−8.
61. Young, J. C., Schneider, C., and Hartl, F. U. (1997) *FEBS Lett. 418*, 139−143.
62. Scheibel, T., Weikl, T., and Buchner, J. (1998) *Proc. Natl. Acad. Sci. U.S.A. 95*, 1495−1499.
63. Young, J. C., Obermann, W. M. J., and Hartl, F. U. (1998) *J. Biol. Chem. 273*, 18007−18010.
64. Soti, C., Radics, L., Yahara, I., and Csermely, P. (1998) *Eur. J. Biochem. 255*, 611−617.

BI983027S